The Astrophysical Journal, 708:L14–L17, 2010 January 1 doi:10.1088/2041-8205/708/1/L14

THE BARYON CONTENT OF COSMIC STRUCTURES

Stacy S. McGaugh[1], James M. Schombert[1], W. J. G. de Blok[1], and Matthew J. Zagursky[1]
[1] Department of Astronomy, University of Maryland, College Park, MD 20742-2421, USA; ssm@astro.umd.edu
[2] Department of Physics, 1274 University of Oregon, Eugene, OR 97403-1274, USA; jschombe@uoregon.edu
[3] Department of Astronomy, University of Cape Town, Private Bag X3, Rondebosch 7701, South Africa; edeblok@ciricnus.ast.uct.ac.za
[4] Institute for Astronomy, University of Hawaii, 2680 Woodlawn Avenue, Honolulu, HI 96826, USA; mzagursk@ifa.hawaii.edu
Received 2009 October 13; accepted 2009 November 18; published 2009 December 11

ABSTRACT

We make an inventory of the baryonic and gravitating mass in structures ranging from the smallest galaxies to rich clusters of galaxies. We find that the fraction of baryons converted to stars reaches a maximum between $M_{500} = 10^{12}$ and $10^{13}\ M_\odot$, suggesting that star formation is most efficient in bright galaxies in groups. The fraction of baryons detected in all forms deviates monotonically from the cosmic baryon fraction as a function of mass. On the largest scales of clusters, most of the expected baryons are detected, while in the smallest dwarf galaxies, fewer than 1% are detected. Where these missing baryons reside is unclear.

Key words: cosmological parameters – dark matter – galaxies: dwarf – galaxies: irregular – galaxies: spiral

1. INTRODUCTION

The early universe was a highly uniform and homogeneous mix of dark and baryonic matter with baryon fraction $f_b = 0.17 \pm 0.01$ (Komatsu et al. 2009). If this primordial mix persists as individual gravitationally bound structures emerge during the course of cosmic evolution, then the baryonic mass of any given object would be $M_b = f_b M_{\rm tot}$. Indeed, combining this with the baryon density constraint from big bang nucleosynthesis (Walker et al. 1991) provides one important argument that the density parameter is less than unity (White et al. 1993; Ostriker & Steinhardt 1995). Here we reverse the logic and ask what fraction of the expected baryons are actually detected.

We present an inventory of the baryonic and gravitating masses of cosmic structures spanning a dozen decades in detected baryonic mass. The mass of baryons known in each system correlates well with the total mass, but not as a simple proportion. The implication is that most of the baryons associated with individual dark matter halos are now missing. While some are in the intergalactic medium (Danforth & Shull 2005), a complete accounting of where the baryons now reside, and how they relate to their parent structures, remains wanting.

2. MASS INVENTORY

We divide our inventory into two broad categories of gravitationally bound systems: those supported by rotation, and those supported by random motions. This distinction is important to the way in which we infer the gravitating mass, as discussed for each type of systems below. The detected baryonic mass is the sum of observed stellar and gaseous components: $M_b = M_* + M_g$. In general, the gas mass is more precisely known as the physics of the emission mechanism is better understood, while the stellar mass requires an estimate of the mass-to-light ratio of a composite stellar population in order to convert observed luminosity to mass. Over the many decades in mass considered here, a factor of ~ 2 uncertainty in the stellar mass-to-light ratio is a minor concern.

2.1. Rotationally Supported Systems

One of the most important lines of evidence for dark matter is the observation that the rotation curves of spiral galaxies tend to become asymptotically flat (Rubin et al. 1978; Bosma 1981) at large radii where the baryonic mass alone should result in a Keplerian decline. This outermost circular velocity, V_c, we take to be representative of the gravitating mass. Among rotating systems, we distinguish between those dominated by stellar mass (typically early-type spirals) and those dominated by gas mass (typically irregular and late-type spirals).

2.1.1. Star-dominated Spiral Galaxies

Bright spiral galaxies have the majority of their detected baryonic mass in the form of stars. We utilize the rotation velocities and mass estimates of McGaugh (2005), selecting only those galaxies with $M_* > M_g$ for $Q = 1$. The results are in good agreement with independent work (de Blok et al. 2008). The sum of baryonic mass is completed by adding the cold gas mass, corrected by a factor of 1.4 to account for the presence of helium and heavier elements. Dust and hot gas do not contribute significantly to the total (Bregman 2007; Anderson & Bregman 2009).

2.1.2. Gas-dominated Galaxies

Many dim, late-type disk galaxies have more of their baryonic mass in the form of atomic gas than in stars: $M_* < M_g$. These are particularly interesting for our purposes here because their baryonic mass is insensitive to the choice of stellar mass estimator. For these galaxies, M_b follows almost directly from the observed 21 cm flux and the physics of the hydrogen hyperfine transition. Two recent independent studies (Stark et al. 2009; Trachternach et al. 2009) provide for the first time a large combined sample of such galaxies.

Rotationally supported disk galaxies are known to obey a relation between baryonic mass and rotation velocity known as the Baryonic Tully–Fisher relation (McGaugh 2005). This is shown in Figure 1, giving emphasis to the gas-dominated galaxies (larger circles) which extend the relation beyond that previously known for bright spirals. They also provide a physics-based calibration of the relation (Stark et al. 2009; Trachternach et al. 2009). This is shown as the dashed line in Figure 1. The intrinsic relation appears to be very tight (Verheijen 2001), with observational uncertainty (due mostly to the uncertainty in the distances to the individual galaxies) accounting for essentially all of the scatter.

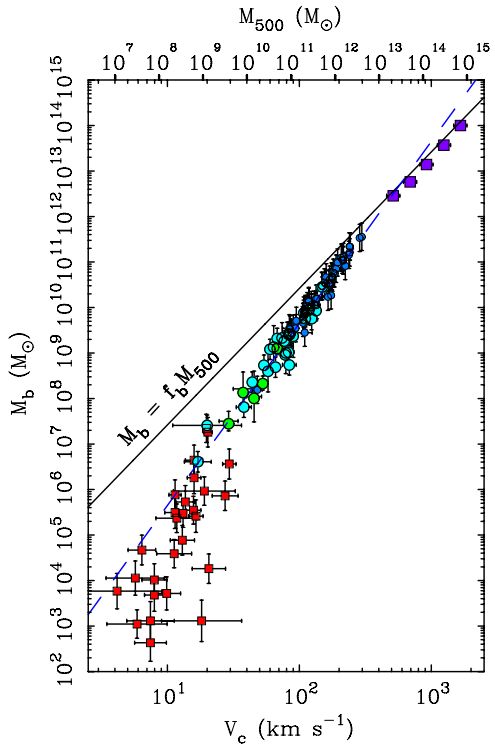

Figure 1. Relation between baryonic mass and rotation velocity. The sum of detected baryonic mass is plotted against the circular velocity of gravitationally bound extragalactic systems. Round symbols represent rotationally supported disks while square symbols represent pressure supported systems. Larger symbols correspond to systems whose baryonic mass is dominated by gas and smaller symbols those dominated by stars. Dark blue circles are for star-dominated spirals (McGaugh 2005). Light blue (Stark et al. 2009) and green (Trachternach et al. 2009) circles represent recent work on gas-dominated disks. Red squares represent Local Group dwarf satellites (Walker et al. 2009). Purple squares represent the mean of many galaxy clusters (Giodini et al. 2009). These pressure-supported systems fall close to, but systematically below the Baryonic Tully–Fisher relation defined by the disks (dashed line). The mass enclosed by an over-density of 500 times the critical density is shown by the upper abscissa assuming $M_{500} = (1.5 \times 10^5\ \mathrm{km^{-3}\ s^3}\ M_\odot^{-1})V_c^3$ (see the discussion in the text). If structures possessed baryons in the cosmic fraction ($f_b = 0.17$), they would fall along the solid line.

The Baryonic Tully–Fisher relation for rotating disks shown in Figure 1 extends over five decades in baryonic mass, a considerable improvement over the two decades typically considered. Before considering how the baryonic mass relates to the total mass, we first investigate whether this relation can be extended still further. Rotationally supported systems cover the range $20 < V_c < 300$ km s^{-1}, but there are both smaller and larger pressure-supported systems.

2.2. Pressure-supported Systems

2.2.1. Elliptical Galaxies

Observations of giant elliptical galaxies typically do not extend far enough radially to identify the equivalent of V_c (Cappellari et al. 2007). Gravitational lensing (Hoekstra et al. 2005; Gavazzi et al. 2007) provides important constraints on the total mass, but the conversion to the equivalent circular velocity is sensitive to the assumed model. It is also subject to degeneracy between stellar and dark masses. Given these uncertainties, and that these data largely overlap with those for spirals, we do not consider giant ellipticals further. We do note that the estimates of Hoekstra et al. (2005) and Gavazzi et al. (2007) are consistent with our results to the same degree that they are consistent with each other.

2.2.2. Local Group Dwarfs

Recent years have witnessed an explosion in the discovery of small satellite galaxies of both the Milky Way (Belokurov et al. 2007) and M31 (McConnachie et al. 2008). The proximity of these quasi-spherical satellite galaxies makes it possible to identify isolated stellar systems much smaller than known elsewhere, and to measure their internal kinematics with velocities from individual stars (Walker et al. 2007, 2009; Simon & Geha 2007). We assume isotropic internal orbits to relate the observed line-of-sight velocity dispersion σ to the circular velocity: $V_c = \sqrt{3}\sigma$ (Wolf et al. 2009). The baryonic masses of these systems are dominated by stars. To convert light to mass, we adopt the mean stellar mass-to-light ratio estimated (Mateo et al. 1998) from resolved stellar population studies: $M_*/L_V = 1.3\,M_\odot/L_\odot$.

2.2.3. Clusters of Galaxies

Recent work (Giodini et al. 2009) on clusters provides a large, homogeneous set of data with stellar, gas, and gravitating masses averaged over many individual clusters. Most of the baryonic mass in clusters is in hot, X-ray-emitting gas. This provides a good measure of both the gas mass and the gravitating mass. Stellar masses are based on a scaling relation (Giodini et al. 2009) derived from K-band data. The result here is not sensitive to the precise relation as the X-ray gas dominates the baryon budget.

It is conventional to refer to structures by the density contrast they represent with respect to the critical density of the universe. The mass enclosed within a radius encompassing the over-density Δ is $M_\Delta = (4\pi/3)\Delta\rho_{\rm crit}R_\Delta^3$. With the definition of critical density and circular velocity, $M_\Delta = (\Delta/2)^{-1/2}(GH_0)^{-1}\ V_\Delta^3$. The cluster data (Giodini et al. 2009) are referenced to $\Delta = 500$, so for $H_0 = 72$ km s^{-1} Mpc^{-1} (Freedman et al. 2001), $M_{500} = (204552\ \mathrm{km^{-3}\ s^3}\ M_\odot^{-1})V_{500}^3$. To relate the circular velocity V_c observed in spirals to V_{500} at larger radii, we note that rotation curves are approximately flat, so we expect $V_c = f_V V_{500}$ with $f_V \approx 1$. If we associate the observed V_c with the peak velocity of a Navarro–Frenk–White (NFW) halo (Navarro et al. 1997), then $1.0 \leqslant f_V \leqslant 1.3$ over the relevant range of masses. This appears consistent with the Milky Way (Flynn et al. 2006; Xue et al. 2008; McGaugh 2008) if $f_V = 1.1$, which we adopt for specificity. This is also consistent with the independent estimate of Lau et al. (2009). Note that a 20% change in f_V corresponds to shifting the cluster data by the width of a data point in Figure 1.

The choice of the radius R_{500} is driven by the data, and is inevitably somewhat arbitrary. A preferable choice might be the virial radius, which occurs around $\Delta \approx 100$ in ΛCDM (Bryan & Norman 1998). The data do not constrain this, nor is there anything genuinely special about the virial radius as the halo profile is expected to merge smoothly with the cosmic background. So we reference our masses to R_{500}, and caution that other plausible choices would give apparently conflicting results merely because of the differing convention. We also note that cluster baryon fractions tend to be rising at the last measured point, which might help us to reconcile them with the cosmic baryon fraction. In contrast, choosing a larger (e.g., virial) reference radius for individual galaxies would only include more dark mass without any additional baryons, driving their inferred baryon fractions to smaller values.

Table 1
Broken Power-law Fit

Scale	Range in V	x	A
Dwarf	<20	8.2	−3.88
Disk	20–350	4.0	1.65
Cluster	>350	3.2	3.69

Note. $\log M_b = x \log V_c + A$.

2.3. Generalized Baryonic Tully–Fisher Relation

Figure 1 represents a generalization of the Baryonic Tully-Fisher relation to pressure-supported systems, and extension to higher and lower masses. The data can be described by a broken power law, with a different slope and normalization at the dwarf, disk galaxy, and cluster scale (Table 1). The variation between these regimes is a small effect compared to the deviation from a constant baryon fraction (solid line in Figure 1). The gravitating mass scales as $M \sim V^3$, but the observed relation is steeper at all scales. Consequently, the detected baryon mass deviates systematically from the expectation of a constant cosmic baryon fraction.

2.4. Binned Data

The data of Giodini et al. (2009) represent the binning of many individual clusters, while the remaining data in Figure 1 represent individual galaxies. To place all data on the same footing, we also bin the galaxy data. We bin in intervals in baryonic mass containing roughly equal numbers of galaxies. We maintain the distinction between galaxies of different types, and for the gas-dominated galaxies, we maintain the separation between the data of Stark et al. (2009) and Trachternach et al. (2009). The binned data are reported in Table 2 and plotted in Figure 2. Table 2 gives the mean and standard deviation in the mean of each logarithmic bin in circular velocity, baryonic mass, stellar mass, and gravitating mass within $\Delta = 500$. It also gives the detected baryon fraction $f_d = M_b/(f_b M_{500})$, which is the ratio of known baryons to the amount expected from the cosmic baryon fraction. The fraction of these nominally available baryons that have been converted into stars is given by the stellar fraction $f_* = M_*/(f_b M_{500})$.

3. DISCUSSION

The stellar fraction reaches a maximum between $M_{500} = 10^{12}$ and $10^{13}\,M_\odot$ (Figure 2). This is broadly consistent with previous results based on counting statistics (Yang et al. 2008). However, there may be some offset in the peak mass scale relating to the long-standing dichotomy between Tully–Fisher and luminosity-function-based normalizations of the halo mass function. Notably, the efficiency of star formation appears to increase monotonically with mass for individual galaxies (Baldry et al. 2008). After the transition to cluster halos containing many galaxies, the efficiency declines again.

Perhaps the most striking aspect of Figure 2 is that the fraction of detected baryons falls short of the cosmic fraction at all scales. In no system is it unity, as would be expected if we had a complete accounting of all the baryons associated with a given bound system. Where are all these missing baryons?

An obvious possibility is that the missing baryons are present, and simply inhabit their dark matter halos in some undetected form. Indeed, one might expect that not all baryons would have time to cool into the observed cold gas and stellar component of galaxies. In this case, many baryons might remain mixed in with the dark halo.

The notion that we are simply not seeing many or even most of the baryons in individual galaxies is profoundly unsatisfactory. Direct searches for hot halo gas have turned up nothing substantial: halo baryon reservoirs fail to explain the observed deficit by two orders of magnitude (Bregman 2007; Anderson & Bregman 2009). In clusters, the hot gas is detected, and constitutes the majority of the baryons. Clusters fall short of the cosmic baryon fraction by a modest amount (McCarthy et al.

Table 2
Binned Data

System	$\langle V_c \rangle$	σ_V	$\langle M_b \rangle$	σ_b	$\langle M_* \rangle$	σ_*	$\langle M_{500} \rangle$	σ_M	f_d	σ_f	f_*	σ_*	Reference
Cluster	3.22	0.05	14.00	0.05	13.13	0.11	14.85	0.15	0.83	0.04	0.11	0.01	1
Cluster	3.10	0.05	13.57	0.07	12.80	0.10	14.48	0.15	0.73	0.05	0.12	0.01	1
Cluster	2.96	0.05	13.14	0.04	12.64	0.11	14.08	0.15	0.68	0.03	0.21	0.02	1
Cluster	2.84	0.05	12.76	0.04	12.36	0.04	13.71	0.15	0.67	0.03	0.26	0.01	1
Cluster	2.71	0.05	12.46	0.21	12.12	0.08	13.32	0.15	0.80	0.16	0.37	0.03	1
Spiral	2.40	0.05	11.32	0.17	11.26	0.14	12.51	0.15	0.38	0.07	0.34	0.05	2
Spiral	2.32	0.03	10.99	0.09	10.94	0.08	12.26	0.08	0.32	0.03	0.28	0.02	2
Spiral	2.23	0.02	10.63	0.09	10.59	0.10	12.01	0.07	0.25	0.02	0.22	0.02	2
Spiral	2.15	0.06	10.26	0.14	10.15	0.20	11.76	0.18	0.19	0.03	0.14	0.03	2
Spiral	2.08	0.04	10.00	0.06	9.85	0.12	11.56	0.11	0.16	0.01	0.11	0.01	2
Gas disk	2.07	0.04	9.85	0.09	9.49	0.09	11.53	0.11	0.12	0.01	0.053	0.005	3
Spiral	2.03	0.02	9.79	0.09	9.62	0.07	11.39	0.07	0.15	0.01	0.10	0.01	2
Spiral	1.92	0.10	9.31	0.46	9.18	0.45	11.06	0.31	0.10	0.05	0.077	0.035	2
Gas disk	1.88	0.05	9.21	0.17	8.61	0.34	10.95	0.16	0.11	0.02	0.027	0.009	3
Gas disk	1.78	0.08	8.62	0.12	7.79	0.37	10.64	0.23	0.057	0.007	0.0083	0.0031	3
Gas disk	1.65	0.14	8.24	0.58	7.12	0.35	10.26	0.42	0.056	0.032	0.0043	0.0015	4
Gas disk	1.37	0.18	7.28	0.44	6.74	0.57	9.42	0.55	0.042	0.019	0.012	0.007	3
Dwarf	1.29	0.10	6.67	0.54	6.67	0.54	9.19	0.29	0.018	0.010	0.018	0.0010	5
Dwarf	1.16	0.13	5.60	0.20	5.60	0.20	8.80	0.38	0.0037	0.0007	0.0037	0.0007	5
Dwarf	0.94	0.20	3.81	0.69	3.81	0.69	8.13	0.60	0.0003	0.0002	0.0003	0.0002	5

Notes. Velocities and masses are logarithmic with units of km s^{-1} and solar masses, respectively.
References. (1) Clusters: Giodini et al. 2009; (2) Spirals: McGaugh 2005; (3) gas-dominated galaxies: Stark et al. 2009; (4) Trachternach et al. 2009; and (5) Local Group dwarfs: Walker et al. 2009.

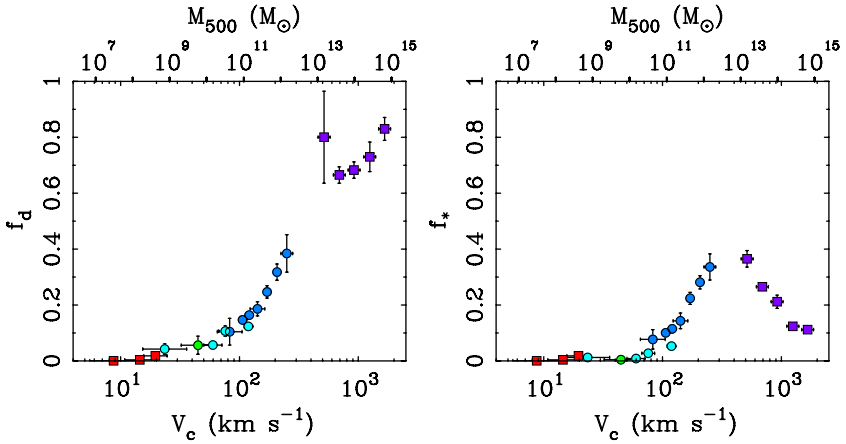

Figure 2. Fraction of the expected baryons that are detected (left: $f_d = M_b/(f_b M_{500})$) and the fraction converted to stars (right: $f_* = M_*/(f_b M_{500})$). Symbols have the same meaning as in Figure 1 but with the binning of Table 2. The detected baryon fraction increases monotonically with mass while the stellar fraction peaks between $M_{500} = 10^{12}$ and $10^{13}\ M_\odot$.

2007; Giodini et al. 2009) which might be readily explicable (Crain et al. 2007). However, the fraction of missing baryons is highly significant on the scales of individual galaxies. In dwarfs, fewer than 1% of the baryons expected from the cosmic fraction are detected.

The detected baryon fraction varies systematically with scale. It is a matter of taste whether one chooses to describe this scale as one of circular velocity, mass, or potential well depth. It is tempting to attribute this correlation to feedback processes being more effective in objects with smaller potential wells (Dekel & Silk 1986). However, the details are heinously complicated (Mayer & Moore 2004; Kereš et al. 2009) and not well understood. We would naively expect feedback to be a messy process resulting in lots of scatter in any correlations that might result. Instead, the observed relation is remarkably tight. In principle, the entire range $0 \leqslant f_d \leqslant 1$ is accessible at each mass, yet only a very particular value is observed. Moreover, the current potential well is the result of the hierarchical assembly of many smaller building blocks. Left to itself, a small dark matter halo will have a small f_d. If incorporated into a larger halo, f_d goes up. How does each building block know to bring the right amount of baryons to the final halo?

We do not see a satisfactory solution to this missing baryon problem at present. Considerable work remains to be done to obtain a complete understanding of the universe and its contents.

The work of S.S.M. is supported in part by NSF grant AST 0505956. M.J.Z. was supported by an REU supplement from the NSF. The work of W.J.G.B. is based upon research supported by the South African Research Chairs Initiative of the Department of Science and Technology and National Research Foundation.

REFERENCES

Anderson, M. E., & Bregman, J. N. 2009, ApJ, submitted
Baldry, I. K., Glazebrook, K., & Driver, S. P. 2008, MNRAS, 388, 945
Belokurov, V., et al. 2007, ApJ, 654, 897
Bosma, A. 1981, AJ, 86, 1791
Bregman, J. N. 2007, ARA&A, 45, 221
Bryan, G. L., & Norman, M. L. 1998, ApJ, 495, 80
Cappellari, M., et al. 2007, MNRAS, 379, 418
Crain, R. A., Eke, V. R., Frenk, C. S., Jenkins, A., McCarthy, I. G., Navarro, J. F., & Pearce, F. R. 2007, MNRAS, 377, 41
Danforth, C. W., & Shull, J. M. 2005, ApJ, 624, 555
de Blok, W. J. G., Walter, F., Brinks, E., Trachternach, C., Oh, S.-H., & Kennicutt, R. C. 2008, AJ, 136, 2648
Dekel, A., & Silk, J. 1986, ApJ, 303, 39
Flynn, C., Holmberg, J., Portinari, L., Fuchs, B., & Jahreiß, H. 2006, MNRAS, 372, 1149
Freedman, W. L., et al. 2001, ApJ, 553, 47
Gavazzi, R., Treu, T., Rhodes, J. D., Koopmans, L. V. E., Bolton, A. S., Burles, S., Massey, R. J., & Moustakas, L. A. 2007, ApJ, 667, 176
Giodini, S., et al. 2009, ApJ, 703, 982
Hoekstra, H., Hsieh, B. C., Yee, H. K. C., Lin, H., & Gladders, M. D. 2005, ApJ, 635, 73
Kereš, D., Katz, N., Davé, R., Fardal, M., & Weinberg, D. H. 2009, MNRAS, 396, 2332
Komatsu, E., et al. 2009, ApJS, 180, 330
Lau, E. T., Nagai, D., & Kravtsov, A. V. 2009, arXiv:0908.2133
Mateo, M., Olszewski, E. W., Vogt, S. S., & Keane, M. J. 1998, AJ, 116, 2315
Mayer, L., & Moore, B. 2004, MNRAS, 354, 477
McCarthy, I. G., Bower, R. G., & Balogh, M. L. 2007, MNRAS, 377, 1457
McConnachie, A. W., et al. 2008, ApJ, 688, 1009
McGaugh, S. S. 2005, ApJ, 632, 859
McGaugh, S. S. 2008, ApJ, 683, 137
Navarro, J. F., Frenk, C. S., & White, S. D. M. 1997, ApJ, 490, 493
Ostriker, J. P., & Steinhardt, P. J. 1995, Nature, 377, 600
Rubin, V. C., Thonnard, N., & Ford, W. K., Jr. 1978, ApJ, 225, L107
Simon, J. D., & Geha, M. 2007, ApJ, 670, 313
Stark, D. V., McGaugh, S. S., & Swaters, R. A. 2009, AJ, 138, 392
Trachternach, C., de Blok, W. J. G., McGaugh, S. S., van der Hulst, J. M., & Dettmar, R.-J. 2009, A&A, 505, 577
Verheijen, M. A. W. 2001, ApJ, 563, 694
Walker, M. G., Mateo, M., Olszewski, E. W., Gnedin, O. Y., Wang, X., Sen, B., & Woodroofe, M. 2007, ApJ, 667, L53
Walker, M. G., Mateo, M., Olszewski, E. W., Peñarrubia, J., Wyn Evans, N., & Gilmore, G. 2009, ApJ, 704, 1274
Walker, T. P., Steigman, G., Kang, H.-S., Schramm, D. M., & Olive, K. A. 1991, ApJ, 376, 51
White, S. D. M., Navarro, J. F., Evrard, A. E., & Frenk, C. S. 1993, Nature, 366, 429
Wolf, J., Martinez, G. D., Bullock, J. S., Kaplinghat, M., Geha, M., Munoz, R. R., Simon, J. D., & Avedo, F. F. 2009, MNRAS, submitted (arXiv:0908.2995)
Xue, X. X., et al. 2008, ApJ, 684, 1143
Yang, X., Mo, H. J., & van den Bosch, F. C. 2008, ApJ, 676, 248